Acta Crystallographica Section C
Crystal Structure Communications
ISSN 0108-2701

Powder X-ray study of racemic (2*RS*,3*RS*)-5-amino-3-(4-phenylpiperazin-1-yl)-1,2,3,4-tetrahydronaphthalen-2-ol

Thaer Assaad and Mwaffak Rukiah*

Department of Chemistry, Atomic Energy Commission of Syria (AECS), PO Box 6091, Damascus, Syrian Arab Republic
Correspondence e-mail: cscientific@aec.org.sy

Received 1 August 2011
Accepted 11 September 2011
Online 15 September 2011

The title compound, $C_{20}H_{25}N_3O$, an important precursor for the preparation of benzovesamicol analogues for the diagnosis of Alzheimer's disease, has been synthesized and characterized by FT–IR, and ^{1}H and ^{13}C NMR spectroscopic analyses. The crystal structure was analysed using powder diffraction as no suitable single crystal was obtained. The piperazine ring has a chair conformation, while the cyclohexene ring assumes a half-chair conformation. The crystal packing is mediated by weak contacts, principally by complementary intermolecular N—H···O hydrogen bonds that connect successive molecules into a chain. Further stabilization is provided by weak C—H···N contacts and by a weak intermolecular C—H···π interaction.

Comment

Racemic (2*RS*,3*RS*)-5-amino-3-(4-phenylpiperazin-1-yl)-1,2,3,4-tetrahydronaphthalen-2-ol, (2*RS*,3*RS*)-(I), is a precursor for the preparation of benzovesamicol analogues which are well known to be stereoselective inhibitors of acetylcholine uptake in presynaptic cholinergic vesicles. Radiolabelled benzovesamicol analogues have been widely used as imaging probes in single photon emission computer tomography (SPECT) and positron emission tomography (PET) *in vitro* and *in vivo* studies of Alzheimer's disease (Alfonso *et al.*, 1993; Efange *et al.*, 1997; Auld *et al.*, 2002; Mulholland & Jung, 1992; Mulholland *et al.*, 1993; Nicolas *et al.*, 2007; Rogers *et al.*, 1989; Zea-Ponce *et al.*, 2005).

The aims of the present study were the synthesis and the three-dimensional structure determination of the title compound, (2*RS*,3*RS*)-(I). The synthesis consisted of the addition of 1-phenylpiperazine to 2,2,2-trifluoro-*N*-(1a,2,7,7a-tetrahydronaphtho[2,3-*b*]oxiren-3-yl)acetamide to obtain two regioisomers, which were separated by flash chromatography (silica gel; Et_2O–Et_3N, 10:1 *v*/*v*) (see Scheme). (2*RS*,3*RS*)-(I) was characterized by IR, and ^{13}C and ^{1}H NMR spectroscopy and yielded results consistent with the assigned structure.

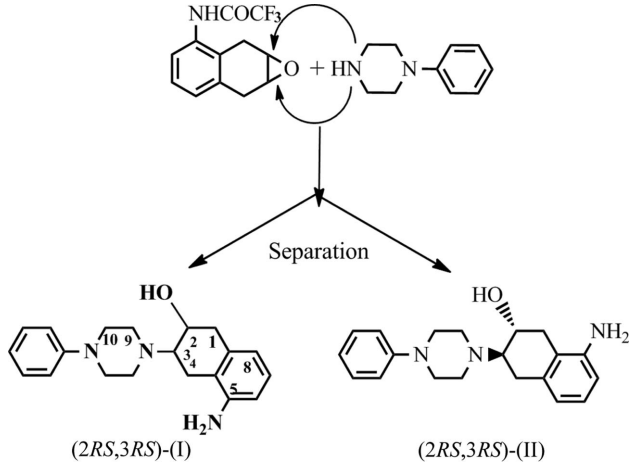

(2*RS*,3*RS*)-(I) crystallizes as a very fine white powder. Since no single crystal of sufficient size and quality was obtained, a structure determination by powder X-ray diffraction was undertaken. In recent years the crystal structures of a number of compounds of pharmaceutical interest have been solved *ab initio* from powder X-ray diffraction data in the absence of single crystals of sufficient quality (Chan *et al.*, 1999; Shankland *et al.*, 2001; Chernyshev *et al.*, 2003; Kiang *et al.*, 2003; Rukiah *et al.*, 2004; van der Lee *et al.*, 2005; Rukiah & Assaad, 2010; Al-Ktaifani & Rukiah, 2010; Rukiah & Al-Ktaifani, 2011). We used in-house powder X-ray diffraction data to solve and refine the crystal structure of (2*RS*,3*RS*)-(I). For a 24-atom (non-H) problem such as this, careful measurement and interpretation are necessary in order to optimize the results.

(2*RS*,3*RS*)-(I) (Fig. 1) crystallizes with one molecule in the asymmetric unit in the space group $P2_1/c$. The molecule contains four six-membered rings (two benzene, a piperazine and a cyclohexene ring). The piperazine ring adopts a chair conformation with puckering parameters (Cremer & Pople, 1975) Q = 0.603 (7) Å, θ = 12.5 (8)° and φ = 195 (2)°. Bond lengths and angles around C14 and C15 (Table 1) confirm the nature of the cyclohexene double bond. The cyclohexene ring

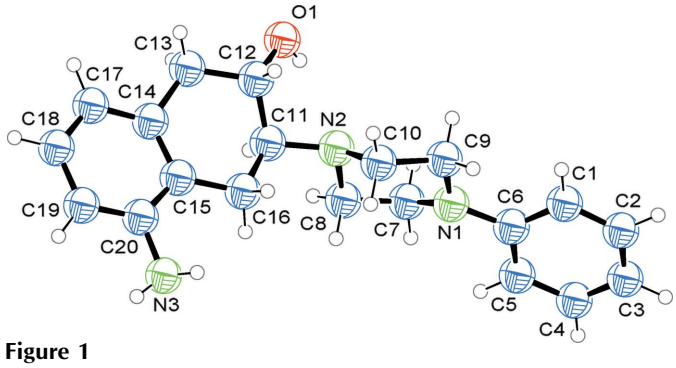

Figure 1
The molecular structure of (2*RS*,3*RS*)-(I), showing the atom numbering. Displacement spheres are drawn at the 50% probability level and H atoms are shown as small spheres of arbitrary radii.

  doi:10.1107/S0108270111036869

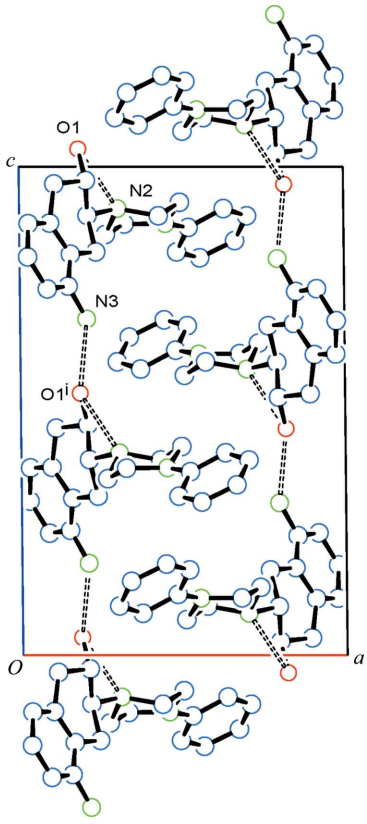

Figure 2
The packing of (2*RS*,3*RS*)-(I), viewed normal to the *b* axis. Intra- and intermolecular O—H···N and N—H···O hydrogen bonds are shown as dashed lines. [Symmetry code: (i) $x, -y-\frac{1}{2}, z-\frac{1}{2}$.]

assumes a conformation approximating a half-chair [puckering parameters Q = 0.471 (7) Å, θ = 54.1 (10)° and φ = 20.7 (12)°], with the C13/C14/C15/C16 atoms nearly coplanar [maximum deviation = 0.148 (6) Å], and C11 and C12 situated 0.319 (7) and 0.283 (7) Å, respectively, on opposite sides of the mean plane. The cyclohexene ring is *trans*-fused to the adjacent benzene ring (C14/C15/C20/C19/C18/C17) through C14 and C15.

As shown in Fig. 2, the most noteworthy noncovalent feature of the structure is an intramolecular contact between a hydroxy H atom and an N atom of the piperazine ring (O1—H1O···N2) (Fig. 2 and Table 2). In this interaction the angle at H is narrow (108°), outside the range normally considered for a hydrogen bond. Atom H1O was observed in a difference map but refined with a bond-length constraint. It is possible that its position is not exact, but in any event the O1—H1O···N2 contact is not a proper hydrogen bond, as the narrow angle signifies that H1O does not present its most electropositive potential in the direction of N2.

The other contacts present (Table 2) have $D\cdots A$ distances at or beyond the sum of the van der Waals radii of the *D* and *A* atoms. N3—H1N3···O1^{i} contacts [symmetry code: (i) $x, -y-\frac{1}{2}, z-\frac{1}{2}$] mediate the formation of chains running in opposite directions along [001] (Fig. 2). C18—H18···N3^{ii} contacts [symmetry code: (ii) $-x, y-\frac{1}{2}, -z+\frac{3}{2}$], between adjacent chains and with amine N3 as acceptor, further

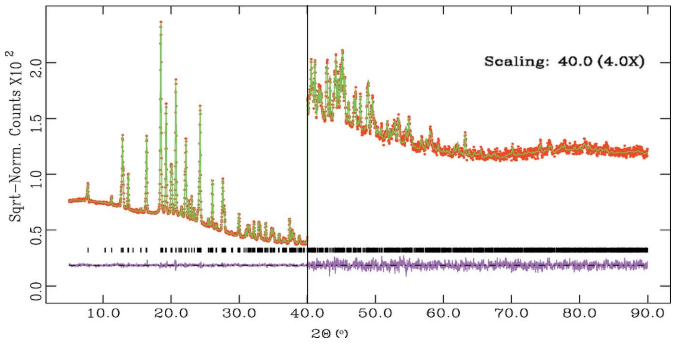

Figure 3
Final Rietveld plot for (2*RS*,3*RS*)-(I). Observed data points are indicated by dots and the best-fit profile (upper trace) and the difference pattern (lower trace) are shown as solid lines. The vertical bars indicate the positions of Bragg peaks.

stabilize the structure. Along the *b* axis, the structure is supported by a weak C7—H7*A*···*Cg*4^{iii} [symmetry code: (iii) $x, y+1, z$] C—H···π interaction, where *Cg*4 is the centre of gravity of the C14/C15/C20/C19/C18/C17 ring. This contact lies near the upper limit of H···*Cg* contact distances for such interactions to be considered significant. We can speculate that the fact that only fine powder is obtained for this compound may be related to the weak packing forces present.

Experimental

2,2,2-Trifluoro-*N*-(1a,2,7,7a-tetrahydronaphtho[2,3-*b*]oxiren-3-yl)acetamide was prepared according to a previously reported method (Rukiah & Assaad, 2010). All other chemicals were obtained commercially and used without further purification. The title compound, (2*RS*,3*RS*)-(I), was prepared by a procedure similar to that reported in the literature (Bando *et al.*, 2000, 2001): 1-phenylpiperazine (3 g, 19 mmol) was added to a solution of 2,2,2-trifluoro-*N*-(1a,2,7,7a-tetrahydronaphtho[2,3-*b*]oxiren-3-yl)acetamide (1.9 g, 7.4 mmol) in ethanol (25 ml). The solution was allowed to reflux for 16 h and was then kept for 24 h at room temperature to produce a crystalline solid. The solid was filtered off and dried under vacuum, then dissolved in methanol (25 ml) and treated with 1 *N* NaOH (15 ml). The mixture was stirred at room temperature for 16 h and then extracted with CH_2Cl_2 (3 × 25 ml). The organic layer was dried over anhydrous Na_2SO_4 and concentrated under reduced pressure. The resulting regioisomers were separated by silica-gel chromatography with Et_2O–Et_3N (10:1 *v*/*v*), giving 665 mg (35%) of (2*RS*,3*RS*)-(I) (R_F = 0.55; m.p. 505 K) and 684 mg (36%) of (2*RS*,3*RS*)-(II) (see Scheme) (R_F = 0.26; m.p. 445 K).

The powder sample of (2*RS*,3*RS*)-(I) was gently ground in a mortar, loaded between two Mylar foils and fixed in the sample holder with a mask of suitable internal diameter (7.0 mm). X-ray powder diffraction data were collected at room temperature with a Stoe Stadi-P diffractometer using monochromatic Cu $K\alpha_1$ radiation (λ = 1.54060 Å) selected with an incident beam curved-crystal germanium (111) monochromator, and using the Stoe transmission geometry (horizontal set-up) with a linear position-sensitive detector (PSD). The pattern was scanned over the angular range 5–90° (2θ).

^{1}H NMR ($CDCl_3$): δ 2.49–2.56 (*m*, 2H, 2H-10), 2.72–3.33 (*m*, 12H, 2H-1, 2H-4, 2H-10, 4H-9, H-3, OH), 3.60 (*s*, NH_2), 3.91–3.97 (*m*, 1H, H-2), 6.57–6.63 (*m*, 2H, H-6, H-8), 6.91 (*t*, 2H, ^3J = 7.2 Hz, $2H_{Ar}$),

6.99–7.04 (*m*, 1H, H-7), 7.28–7.33 (*m*, 3H, $3H_{Ar}$).^{13}C NMR ($CDCl_3$): δ 20.9 (2 C-10), 38.0 (C-1), 48.1 (C-4), 49.9 (C-3), 65.2 (C-2), 66.2 (2 C-9), 112.7 (CH_{Ar}), 116.3 (2 CH_{Ar}), 119.3 (C_{Ar}), 119.6 (CH_{Ar}), 120.0 (CH_{Ar}), 127.1 (CH_{Ar}), 129.1 (2 CH_{Ar}), 134.7 (C_{Ar}), 144.4 (C—NH_2), 151.2 (C_{Ar}). IR (KBr, ν cm^{-1}): 3200–3350.4 (NH_2), 3459.5 (OH), 3050 (CH═CH, Ar), 2918.2–2850.9 (CH_2, aliphatic), 2850.9 (CH_2—NH_2), 1636.6 (C═C), 1137.6 (C—N, piperazine).

Crystal data

$C_{20}H_{25}N_3O$
M_r = 323.44
Monoclinic, $P2_1/c$
a = 11.4132 (4) Å
b = 8.8555 (3) Å
c = 17.1797 (4) Å
β = 90.5787 (17)°
V = 1736.27 (9) Å^3
Z = 4
Cu $K\alpha_1$ radiation
λ = 1.5406 Å
μ = 0.61 mm^{-1}
T = 298 K
Flat sheet, 7 × 7 mm

Data collection

Stoe transmission Stadi-P diffractometer
Specimen mounting: powder loaded between two Mylar foils
Data collection mode: transmission
Scan method: step
Absorption correction: for a cylinder mounted on the φ axis (*GSAS*; Larson & Von Dreele, 2004)
T_{min} = 0.653, T_{max} = 0.664
$2\theta_{min}$ = 4.972°, $2\theta_{max}$ = 89.952°, $2\theta_{step}$ = 0.02°

Refinement

R_p = 0.020
R_{wp} = 0.027
R_{exp} = 0.020
R_{Bragg} = ?
$R(F)$ = ?
$R(F^2)$ = 0.07470
χ^2 = 1.877
4250 data points
190 parameters
29 restraints
H-atom parameters constrained

For pattern indexing, the extraction of the peak positions was carried out with the program *WinPLOTR* (Roisnel & Rodriguez-Carvajal, 2001). Pattern indexing was performed with the program *DicVol4.0* (Boultif & Louër, 2004). The first 20 lines were completely indexed on the basis of a monoclinic cell. The absolute error on each observed line was fixed at 0.02° (2θ). The figures of merit [$M(20)$ = 17.9 and $F(20)$ = 36.6] are sufficient to support the results obtained. The entire powder diffraction pattern from 5 to 90° (2θ) was subsequently refined with cell and resolution constraints (Le Bail *et al.*, 1988) using a monoclinic space group without systematic absences, *P*2/*m*, *via* the 'profile matching' option of the program *FULLPROF* (Rodriguez-Carvajal, 2001). The monoclinic space group $P2_1/c$ was chosen with the help of the program *Check Group* interfaced by *WinPLOTR*. The number of molecules per unit cell was estimated to be Z = 4, giving Z' = 1 molecule per asymmetric unit for this space group. Structure solution was attempted *ab initio* by direct methods using the program *EXPO2004* (Altomare *et al.*, 2004), but was not successful. Therefore, the direct space method was used (*FOX*; Favre-Nicolin & Černý, 2002) for finding the starting model. It is worth pointing out that *FOX* solves structures by altering the positions, orientations and conformations of the molecule(s) in the unit cell according to the constraints of space-group symmetry, until a good match is obtained between the calculated and observed intensities. The starting model was found using the 'parallel tempering' algorithm of the Monte Carlo simulated annealing method. The 2θ angular range was restricted to 5.0–55.0° to speed up the Monte Carlo calculations. The profile parameter needed for the program was calculated from preliminary profile-matching refinements carried out with the program *FOX* itself. During the Monte Carlo simulated annealing calculations, each molecule was allowed to translate, to rotate around its centre of mass and to have its torsion angles vary. (2*RS*,3*RS*)-(I) has two independent torsion angles, so there are eight degrees of freedom to determine for the starting model. The H atoms were not included at this stage. After roughly one million cycles, the agreement factor R_{wp} was near 10% for a solution corresponding to a configuration which provided a credible starting model in terms of crystal packing. The shortest contact distance between neighbouring molecules was 3.15 Å between a hydroxy O and a neighbouring amine N atom, representing a possible hydrogen-bond distance.

The model found by this program was introduced in the program *GSAS* (Larson & Von Dreele, 2004) implemented in *EXPGUI* (Toby, 2001) for Rietveld refinements. The effect of the asymmetry of low-order peaks was corrected using a pseudo-Voigt description of the peak shape (Thompson *et al.*, 1987) which allows for angle-dependent asymmetry with axial divergence (Finger *et al.*, 1994). The two asymmetry parameters of this function *S*/*L* and *D*/*L* were both fixed at 0.0215 during the Rietveld refinement. All bond lengths involving the 24 non-H atoms were restrained to the values normally found in similar chemical environments, as taken from Allen *et al.* (1987). Unit weights were used for these restraints. A global isotropic atomic displacement parameter was introduced for C, N and O atoms. Intensities were corrected for absorption effects with a $\mu.d$ value of 0.164. Before the final refinement, aromatic, methylene and methine H atoms were introduced at calculated positions (aromatic and methine C—H = 0.99 Å and methylene C—H = 0.98 Å). These H atoms were treated as riding. The H atoms of the hydroxy and amine groups were located in a difference Fourier synthesis and refined with constrained bond lengths (O—H = 0.82 Å and N—H = 0.87 Å) and angles. A spherical harmonic correction for preferred orientation (Von Dreele, 1997) was applied in the final refinement, with 16 coefficients. The use of the preferred orientation correction leads to better molecular geometry and better agreement factors. The final Rietveld plot of the X-ray diffraction pattern is given in Fig. 3.

Data collection: *WinXPOW* (Stoe & Cie, 1999); cell refinement: *GSAS* (Larson & Von Dreele, 2004); data reduction: *WinXPOW*; program(s) used to solve structure: *FOX* (Favre-Nicolin & Černý, 2002); program(s) used to refine structure: *GSAS*; molecular

Table 1
Selected geometric parameters (Å, °).

C13—C14	1.520 (9)	C15—C16	1.493 (10)
C14—C15	1.402 (10)		
C13—C14—C15	120.9 (9)	C14—C15—C16	122.9 (9)
C15—C14—C17	123.8 (8)	C14—C15—C20	113.2 (10)
C7—N1—C6—C5	−38.1 (12)	C13—C14—C15—C20	169.3 (8)
C8—N2—C11—C12	−154.5 (5)	C17—C14—C15—C16	−174.2 (9)

Table 2
Hydrogen-bond geometry (Å, °).

*Cg*4 is the centre of gravity of the C14/C15/C20/C19/C18/C17 ring.

D—H···*A*	*D*—H	H···*A*	*D*···*A*	*D*—H···*A*
O1—H1O···N2	0.82	2.33	2.698 (12)	108
N3—H1N3···O1^{i}	0.87	2.26	3.112 (8)	166
C18—H18···N3^{ii}	0.99	2.60	3.537 (11)	158
C7—H7*A*···*Cg*4^{iii}	0.98	2.88	3.605 (6)	132

Symmetry codes: (i) $x, -y-\frac{1}{2}, z-\frac{1}{2}$; (ii) $-x, y-\frac{1}{2}, -z+\frac{3}{2}$; (iii) $x, y+1, z$.

graphics: *ORTEP* (Farrugia, 1997); software used to prepare material for publication: *publCIF* (Westrip, 2010).

The authors thank Professors I. Othman, Director General, and T. Yassine, Head of Chemistry Department, Atomic Energy Commission of Syria, for their support and encouragement.

Supplementary data for this paper are available from the IUCr electronic archives (Reference: FA3258). Services for accessing these data are described at the back of the journal.

References

Alfonso, A., Grundahl, K., Duerr, J. S., Han, H. P. & Rand, J. B. (1993). *Science*, **261**, 617–619.

Al-Ktaifani, M. & Rukiah, M. (2010). *Acta Cryst.* C**66**, o479–o483.

Allen, F. H., Kennard, O., Watson, D. G., Brammer, L., Orpen, A. G. & Taylor, R. (1987). *J. Chem. Soc. Perkin Trans. 2*, pp. S1–19.

Altomare, A., Caliandro, R., Camalli, M., Cuocci, C., Giacovazzo, C., Moliterni, A. G. G. & Rizzi, R. (2004). *J. Appl. Cryst.* **37**, 1025–1028.

Auld, D. S., Kornecook, T. J., Bastianetto, S. & Quirion, R. (2002). *Prog. Neurobiol.* **68**, 209–245.

Bando, K., Naganuma, T., Taguchi, K., Ginoza, Y., Tanaka, Y., Koike, K. & Takatoku, K. (2000). *Synapse*, **38**, 27–37.

Bando, K., Taguchi, K., Ginoza, Y., Naganuma, T., Tanaka, Y., Koike, K. & Takatoku, K. (2001). *Nucl. Med. Biol.* **28**, 251–260.

Boultif, A. & Louër, D. (2004). *J. Appl. Cryst.* **37**, 724–731.

Chan, F. C., Anwar, J., Cernik, R., Barnes, P. & Wilson, R. M. (1999). *J. Appl. Cryst.* **32**, 436–441.

Chernyshev, V. V., Machon, D., Fitch, A. N., Zaitsev, S. A., Yatsenko, A. V., Shmakov, A. N. & Weber, H.-P. (2003). *Acta Cryst.* B**59**, 787–793.

Cremer, D. & Pople, J. A. (1975). *J. Am. Chem. Soc.* **97**, 1354–1358.

Efange, S. M. N., Garland, E., Staley, J. K., Khare, A. B. & Mash, D. C. (1997). *Neurobiol. Aging*, **18**, 407–413.

Farrugia, L. J. (1997). *J. Appl. Cryst.* **30**, 565.

Favre-Nicolin, V. & Černý, R. (2002). *J. Appl. Cryst.* **35**, 734–743.

Finger, L. W., Cox, D. E. & Jephcoat, A. P. (1994). *J. Appl. Cryst.* **27**, 892–900.

Kiang, Y. H., Huq, A., Stephens, P. W. & Xu, W. (2003). *J. Pharm. Sci.* **92**, 1844–1853.

Larson, A. C. & Von Dreele, R. B. (2004). *GSAS*. Report LAUR 86-748. Los Alamos National Laboratory, New Mexico, USA.

Le Bail, A., Duroy, H. & Fourquet, J. L. (1988). *Mater. Res. Bull.* **23**, 447–452.

Lee, A. van der, Richez, P. & Tapiero, C. (2005). *J. Mol. Struct.* **743**, 223–228.

Mulholland, G. K. & Jung, Y. W. (1992). *J. Labelled Comp. Radiopharm.* **31**, 253–259.

Mulholland, G. K., Jung, Y. W., Wieland, D. M., Kilbourn, M. R. & Kuhl, D. E. (1993). *J. Labelled Comp. Radiopharm.* **33**, 583–591.

Nicolas, G., Patrick, E., Roger, R. F., David, J. H., Sylvie, C., Lucette, G., Peter, R., Stefan, E., Sylvie, M., Sylvie, B., Michael, J. F., Denis, G. & Michael, K. (2007). *Synapse*, **61**, 962–970.

Rodriguez-Carvajal, J. (2001). *FULLPROF*. CEA/Saclay, France.

Rogers, G. A., Parsons, S. M., Anderson, D. C., Nilsson, L. M., Bahr, B. A., Kornreich, W. D., Kaufman, R., Jacobs, R. S. & Kirtman, B. (1989). *J. Med. Chem.* **32**, 1217–1230.

Roisnel, T. & Rodriguez-Carvajal, J. (2001). *Mater. Sci. Forum*, **378–381**, 118–123.

Rukiah, M. & Al-Ktaifani, M. (2011). *Acta Cryst.* C**67**, o166–o170.

Rukiah, M. & Assaad, T. (2010). *Acta Cryst.* C**66**, o475–o478.

Rukiah, M., Lefebvre, J., Hernandez, O., van Beek, W. & Serpelloni, M. (2004). *J. Appl. Cryst.* **37**, 766–772.

Shankland, N., David, W. I. F., Shankland, K., Kennedy, A. R., Frampton, C. S. & Florence, A. J. (2001). *Chem. Commun.* pp. 2204–2205.

Stoe & Cie (1999). *WinXPOW*. Stoe & Cie, Darmstadt, Germany.

Thompson, P., Cox, D. E. & Hastings, J. B. (1987). *J. Appl. Cryst.* **20**, 79–83.

Toby, B. H. (2001). *J. Appl. Cryst.* **34**, 210–213.

Von Dreele, R. B. (1997). *J. Appl. Cryst.* **30**, 517–525.

Westrip, S. P. (2010). *J. Appl. Cryst.* **43**, 920–925.

Zea-Ponce, Y., Mavel, S., Assaad, T., Kruse, S. E., Parsons, S. M., Emond, P., Chalon, S., Kruse, S., Giboureau, N., Kassiou, M. & Guilloteau, D. (2005). *Bioorg. Med. Chem.* **13**, 745–753.